

# On the solution of the three forces problem and its application in optimal designing of a class of symmetric plane frameworks of least weight

Tomasz Sokół · Tomasz Lewiński

Received: 17 April 2010 / Revised: 15 July 2010 / Accepted: 25 July 2010 / Published online: 12 August 2010  
© The Author(s) 2010. This article is published with open access at Springerlink.com

**Abstract** Two problems of minimum weight design of plane trusses are dealt with. The first problem concerns construction of the lightest fully stressed truss subject to three self-equilibrated forces applied at three given points. This problem has been solved analytically by H.S.Y. Chan in 1966. This analytical solution is re-derived in the present paper. It compares favourably with new numerical solutions found here by the method developed recently by the first author. The solution to the three forces problem paves the way to half-analytical as well as numerical solutions to the problem of minimum weight design of plane symmetric frameworks transmitting two symmetrically located vertical forces to two fixed supports lying along the line linking the points of application of the forces.

**Keywords** Minimum weight design · Michell trusses · Interior point method

## 1 Introduction

The aim of the present paper is twofold. The first part deals with theoretical construction of the fully stressed and the lightest plane trusses subjected to three self-equilibrated

co-planar forces applied at three given points. This problem will not be solved completely, it involves many parameters. Nevertheless, an important class of its solutions, belonging to the Michell (1904) class, will be considered. Solution of this problem will make it possible to solve a minimum weight design problem of fully stressed symmetric frameworks transmitting two vertical forces to two fixed hinge supports lying on the line of application of the forces.

The three-forces problem was discussed by Chan (1960), this report being unavailable for the present authors, and these results are cited in Hemp (1973) and in the reports by Chan (1963, 1964, 1966), being available for the present authors. Some suggestions of how to solve the three-forces problem can be found in Dewhurst (2001) and Melchers (2005). Some continuum based layouts are predicted by Golay and Seppecher (2001, Section 5). In the present paper we shall draw upon the methods developed by Chan (1966) in a report-to the best of the present authors' knowledge never cited till now, including the book by Hemp (1973) and other papers by H.S.Y. Chan (1963, 1964, 1967, 1975). The results of Chan (1966) will be re-derived here with using the notation and some new ideas developed in Lewiński et al. (1994a, b), Graczykowski and Lewiński (2006a, b, c, 2007a, b), Rozvany (1998) and Lewiński and Rozvany (2007, 2008a, b). It is thought appropriate to deliver a possibly complete derivation of all the formulae describing the three-forces problem, because they will be useful in the construction of new analytical solutions to other optimum design problems within the theory of Michell trusses. The minimal weight of the truss subject to the three given forces will be found here by the kinematic method with using the virtual displacements slightly different than those used by Chan (1966). The construction of the virtual displacement fields is rather complex and that is why it is presented here

---

T. Sokół (✉) · T. Lewiński  
Department of Structural Mechanics and Computer Aided  
Engineering, Faculty of Civil Engineering,  
Warsaw University of Technology, Al.Arмии Ludowej 16,  
00-637 Warsaw, Poland  
e-mail: T.Sokol@il.pw.edu.pl

T. Lewiński  
e-mail: T.Lewinski@il.pw.edu.pl

with all details to make the paper readable. The problems discussed in the paper are of fundamental importance for the theory of optimum design of structures, hence they deserve such a detailed treatment.

The analytically found layouts of Michell trusses equilibrating a given system of three forces are compared with numerical solutions found by the method developed recently by Sokół (2010). This numerical method is based on the linear programming formulation of the problem of optimum design of fully stressed trusses of finite number of bars, discussed already in Hemp (1973, Ch. 1), Achtziger (1997) and Gilbert and Tyas (2003). The new ideas lie in the proper programming of the problem and in the specific usage of the Mathematica package. The large linear programming problems were effectively solved using the interior point method with sparse matrix representation. The numerical solutions lie very closely to the analytical results, which proves correctness of both the analytical and numerical predictions.

The layouts which solve the three-forces problem are components of the more complex Michell solutions. In the present paper these layouts will be used to construct the optimal shapes of the lightest fully stressed frameworks transmitting two vertical forces to the fixed supports lying on the line linking the points of application of the applied forces. This self-equilibrated system of two vertical forces and two reactions is assumed to be symmetric, see Fig. 16. The layout concerning the three-forces problem determines the solutions around the supports. The reactions are oblique—they are transmitted to the curved reinforcing bar which becomes straight in the middle part of the structure, and where it is the only solid member of the solution. The applied vertical forces are transmitted by the fans of infinitely thin bars which transmit the vertical force to the upper curved bar in such a manner that this bar is not bent. Two methods of construction of the considered optimal solution are presented. In the first method a one parameter family of layouts is considered, the optimal one being chosen from the condition of minimum weight. In the second method a certain auxiliary saddle point problem is formulated, its solution being just the solution characterized by the minimal weight. The latter method results in an explicit form of the set of equations, whose solution determines the unknown design variables. Thus the solutions constructed in this manner can be viewed as half-analytic. We show that they almost coincide with the approximate solutions found by the direct numerical method of Sokół (2010). Similar layouts for this problem have also been predicted by other numerical methods, also those based on the continuum formulation with additional techniques of filtering, like SIMP, see the results by Lógó et al. (2009).

## 2 The three forces problem

### 2.1 Formulation

Let three points: R, N, D are given. In this plane we introduce the Cartesian coordinate system  $(x, y)$  of origin R, the  $x$  axis being directed along RN, see Fig. 1. The points R, N, D will be nodes of the unknown framework. Only these nodes are subject to the forces:  $\mathbf{P} = (P_x, P_y)$ ,  $\mathbf{Q} = (Q_x, Q_y)$ ,  $\mathbf{F} = (F_x, F_y)$ . Without loss of generality one of the nodes—the node R—can be assumed to be fixed. Thus the force at R will be viewed as the reaction  $\mathbf{P} = (P_x, P_y)$ , see Fig. 1.

Our task is to find the lightest framework subjected to the forces  $\mathbf{P}, \mathbf{F}, \mathbf{Q}$  at the nodes R, D, N, respectively, of the areas of cross-sections chosen such that the axial stress in the members is bounded from both sides as follows:  $-\sigma_p \leq \sigma \leq \sigma_p$ .

It will occur that in all members the equality:  $|\sigma| = \sigma_p$  is attained, which means that the bars are uniformly stressed.

In the present paper we confine our attention to the subclass of the problem of three forces given by the layouts consisting of two circular fans: RBA (of radius  $r_2$ ) and NAC (of radius  $r_1$ ) and of a fibrous domain ABDC, composed of two families of curvilinear and orthogonal fibres. The force  $\mathbf{F}$  at D induces the forces in the bars BD and CD of different signs. Thus the resultant of the components  $F_x, F_y$  must lie within the dashed lines around D. This sub-class of solutions of the problem of three forces was discovered by Chan (1966). To make the present paper self-contained we shall outline the method of Chan of finding the angular parameters

$$\gamma_1 = \angle RNA, \quad \theta_1 = \angle ANC, \quad \theta_2 = \angle BRA \quad (2.1)$$

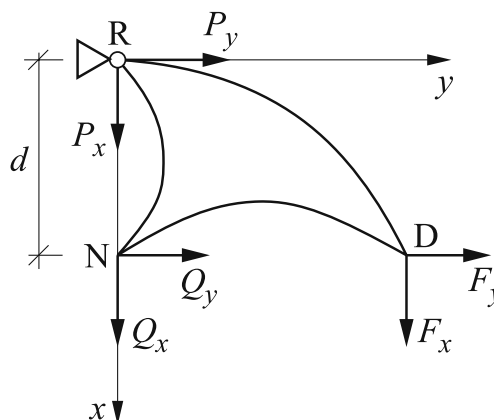


Fig. 1 The problem setting

which describe geometry of the whole fibrous domain RBDCNAR.

### 2.2 Geometry of the domain RBDCNAR

The arcs AC and AB have circular shapes, the radii being

$$\begin{aligned} r_1 &= |NA| = |NC| \\ r_2 &= |RA| = |RB| \end{aligned} \tag{2.2}$$

and can be expressed by the angles  $\gamma_1, \gamma_2$

$$r_1 = d \cos \gamma_1, \quad r_2 = d \cos \gamma_2 \tag{2.3}$$

where  $\gamma_1 + \gamma_2 = \frac{\pi}{2}$ ; the distance  $d = |RN|$  being given. The sides RA and NA of the right angled triangle RAN determine a Cartesian coordinate system  $(x_0, y_0)$  of origin at A. The domain ABDC is parameterized by a curvilinear orthogonal system  $(\alpha, \beta)$ . The coordinates  $(\alpha, \beta)$  of the vertices of this domain are

$$A(0, 0), \quad C(\theta_1, 0), \quad B(0, \theta_2), \quad D(\theta_1, \theta_2)$$

The analytical construction of the  $(\alpha, \beta)$  net has been for the first time developed by Carathéodory and Schmidt (1923) and then by Chan (1964). The Lamé coefficients at an arbitrary point  $(\lambda, \mu)$ , referring to the given curvilinear parameterization are expressed by the formulae

$$\begin{aligned} A(\lambda, \mu) &= r_1 G_0(\lambda, \mu) + r_2 G_1(\mu, \lambda) \\ B(\lambda, \mu) &= r_2 G_0(\lambda, \mu) + r_1 G_1(\lambda, \mu) \end{aligned} \tag{2.4}$$

cf. (6.7) and (6.8) in Graczykowski and Lewiński (2006a); the functions  $G_n(\lambda, \mu)$  are defined by (1) in Lewiński et al. (1994a). Let us define the functions

$$\begin{aligned} \bar{x}(\lambda, \mu) &= r_1 F_1(\lambda, \mu) + r_2 F_2(\mu, \lambda) \\ \bar{y}(\lambda, \mu) &= r_1 F_2(\lambda, \mu) + r_2 F_1(\mu, \lambda) \end{aligned} \tag{2.5}$$

where  $F_n(\lambda, \mu)$  are given by (2) in Lewiński et al. (1994a). Let

$$\phi(\lambda, \mu) = \mu - \lambda \tag{2.6}$$

The Cartesian coordinates  $(x^o, y^o)$  of a point  $(\lambda, \mu)$  are

$$\begin{aligned} x^o(\lambda, \mu) &= \bar{x}(\lambda, \mu) \cos(\phi(\lambda, \mu)) \\ &\quad - \bar{y}(\lambda, \mu) \sin(\phi(\lambda, \mu)) \\ y^o(\lambda, \mu) &= \bar{x}(\lambda, \mu) \sin(\phi(\lambda, \mu)) \\ &\quad + \bar{y}(\lambda, \mu) \cos(\phi(\lambda, \mu)) \end{aligned} \tag{2.7}$$

see (6.16) in Graczykowski and Lewiński (2006a). The coordinates  $(x, y)$  of point  $(\lambda, \mu)$  are given by

$$\begin{aligned} x(\lambda, \mu) &= [x^o(\lambda, \mu) + r_2] \cos \gamma_2 \\ &\quad - y^o(\lambda, \mu) \sin \gamma_2 \\ y(\lambda, \mu) &= [x^o(\lambda, \mu) + r_2] \sin \gamma_2 \\ &\quad + y^o(\lambda, \mu) \cos \gamma_2 \end{aligned} \tag{2.8}$$

and just with using these formulae the net of lines in Fig. 2 was constructed.

By using (2.3) and (7)–(14) in Lewiński et al. (1994a) one can rearrange (2.8) to the form

$$\begin{aligned} \frac{x(\lambda, \mu)}{d} &= \sin \gamma_2 k_1(\lambda, \mu) - \cos \gamma_2 k_2(\lambda, \mu) \\ \frac{y(\lambda, \mu)}{d} &= -\sin \gamma_2 h_1(\lambda, \mu) + \cos \gamma_2 h_2(\lambda, \mu) \end{aligned} \tag{2.9}$$

with

$$\begin{aligned} h_1(\lambda, \mu) &= -\cos(\gamma_2 + \phi(\lambda, \mu)) F_2(\lambda, \mu) \\ &\quad - \sin(\gamma_2 + \phi(\lambda, \mu)) F_1(\lambda, \mu) \\ h_2(\lambda, \mu) &= \cos(\gamma_2 + \phi(\lambda, \mu)) F_1(\lambda, \mu) \\ &\quad + \sin(\gamma_2 + \phi(\lambda, \mu)) F_0(\lambda, \mu) \end{aligned} \tag{2.10}$$

and

$$\begin{aligned} k_1(\lambda, \mu) &= -\sin(\gamma_2 + \phi(\lambda, \mu)) F_2(\lambda, \mu) \\ &\quad + \cos(\gamma_2 + \phi(\lambda, \mu)) F_1(\lambda, \mu) \\ k_2(\lambda, \mu) &= \sin(\gamma_2 + \phi(\lambda, \mu)) F_1(\lambda, \mu) \\ &\quad - \cos(\gamma_2 + \phi(\lambda, \mu)) F_0(\lambda, \mu) \end{aligned} \tag{2.11}$$

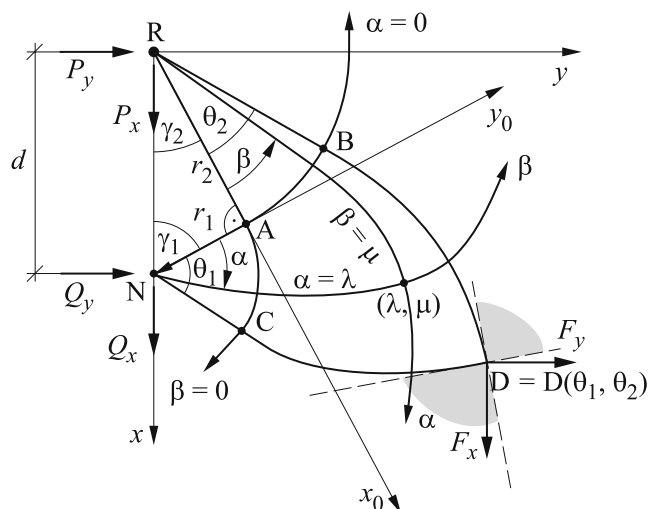


**Fig. 2** Parameterization of the fans RBA, NAC and the fibrous domain ABDC

### 2.3 Computation of the reactions at node N

Let  $x_D = x(\theta_1, \theta_2)$ ,  $y_D = y(\theta_1, \theta_2)$  be coordinates of point D in the coordinate system  $(x, y)$  of origin at R.

Let us write down the equilibrium equations involving the reactions  $Q_x, Q_y$  at node N. The condition of vanishing of the moment of external forces with respect to the hinge R reads

$$-dQ_y - x_D F_y + y_D F_x = 0 \tag{2.12}$$

We need one formula more to find the reactions  $Q_x$  and  $Q_y$ . There are two manners to find such a formula. The first, natural way is very laborious—one should solve the equilibrium problem of the domain ABDC, starting from the equilibrium equations of the node D. These two equilibrium equations result in the values of the axial forces in bars BD and CD. Having found these axial forces (which are constant along the boundary lines DB, DC) one can solve the equilibrium problem of the interior of the domain ABDC, i.e. find the internal forces in the meaning of Hemp (1973) by following the method developed in Graczykowski and Lewiński (2007a). These internal forces are defined by

$$T_1 = BN_I, \quad T_2 = AN_{II} \tag{2.13}$$

where  $N_I$  and  $N_{II}$  are the principal stress resultants within the theory of plane stress; the principal directions  $(I, II)$  coincide with the  $(\alpha, \beta)$  trajectories. Having the forces  $T_1$  and  $T_2$  along AC one can find the distribution of  $T_2$  within the fan NAC and then the resultant of these forces at N, being the reaction  $Q$ . The component  $Q_y$  thus obtained will coincide with the solution of the algebraic equation (2.12). Additionally we shall be able to compute the component  $Q_x$ .

Much shorter way of computing  $Q_x$  was proposed by Chan (1966). One should make use of the variational equation of equilibrium, cf. (6.1) in Graczykowski and Lewiński (2007b):

$$\iint \left[ T_1 \left( \frac{\partial u}{\partial \alpha} + v \right) + T_2 \left( \frac{\partial v}{\partial \beta} + u \right) \right] d\alpha d\beta + \mathcal{L}_{NCD} + \mathcal{L}_{RBD} = \mathcal{L}(u, v) \tag{2.14}$$

where  $u(\alpha, \beta), v(\alpha, \beta)$  are components of the virtual displacements (referred to the  $(\alpha, \beta)$  parameterization) the integration being taken over the whole structure. The linear form  $\mathcal{L}(u, v)$  represents the virtual work of the loading. In the case considered the structure contains two bars (RBD and NCD) of finite cross sections and that is why the left hand side of (2.14) is complemented by  $\mathcal{L}_{NCD} + \mathcal{L}_{RBD}$ —the virtual work of axial forces in these bars on the axial deformations, like in (2.5) of Graczykowski and Lewiński (2006a).

Now we choose the fields  $u$  and  $v$  in such a manner that the left hand side of (2.14) vanishes

$$\frac{\partial u}{\partial \alpha} + v = 0, \quad \frac{\partial v}{\partial \beta} + u = 0 \tag{2.15}$$

Then the axial deformations along the fibres  $\alpha$  and  $\beta$  vanish; consequently, the virtual works  $\mathcal{L}_{NCD}$  and  $\mathcal{L}_{RBD}$  assume zero values. We shall assume additionally that

$$\varepsilon_{r\vartheta} = 0 \text{ in NCA, RBA} \tag{2.16}$$

The virtual work represented by the right-hand side of (2.14) comprises the virtual work of reactions  $P_x$  and  $P_y$ . To make this virtual work zero it is assumed that

$$u(R) = 0, \quad v(R) = 0 \tag{2.17}$$

It will turn out that the family of fields  $(u, v)$  satisfying (2.15) and (2.16) is two-parameter—it depends on two independent constants. Thus the (2.14) will imply two algebraic equilibrium equations. These two equations imply (2.12) and, additionally, an equation linking  $Q_x, F_x$  and  $F_y$ . It was already mentioned that this second equation cannot be easily inferred from the equilibrium equations. Therefore, the kinematic method proposed by Chan (1966) will turn out to be especially effective in the problem discussed.

Let us turn to the details. We shall construct the kinematic fields  $u, v$  satisfying the conditions (2.15) within ABDC, the conditions of vanishing of the radial and circumferential strains within the fans RBA and NAC, the continuity conditions as well as the conditions (2.16). We start with construction of these fields in the fan RBA.

The polar coordinates are denoted by  $(r, \vartheta)$ , the fields  $u, v$  being measured along these directions, cf. Fig. 3. Let us recall the formulae defining the strain components in the polar system

$$\varepsilon_r = \frac{\partial u}{\partial r}, \quad \varepsilon_\vartheta = \frac{u}{r} + \frac{1}{r} \frac{\partial v}{\partial \vartheta}, \tag{2.18}$$

$$2\varepsilon_{r\vartheta} = \frac{1}{r} \frac{\partial u}{\partial \vartheta} + \frac{\partial v}{\partial r} - \frac{v}{r}$$

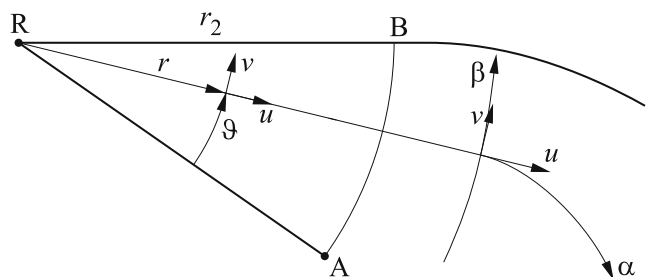


Fig. 3 The polar parameterization within RBA

The conditions

$$\varepsilon_r = 0, \quad \varepsilon_\vartheta = 0, \quad \varepsilon_{r\vartheta} = 0 \tag{2.19}$$

imply the following representation of the displacement fields

$$\begin{aligned} u^{\text{RAB}} &= \bar{C}_1 \cos(\vartheta - \bar{\varphi}), \\ v^{\text{RAB}} &= \bar{\psi}r - \bar{C}_1 \sin(\vartheta - \bar{\varphi}) \end{aligned} \tag{2.20}$$

These equations follow from (77) of Lewiński and Rozvany (2007), where  $\epsilon = 0$  was put. Here  $\bar{C}_1, \bar{\psi}, \bar{\varphi}$  are arbitrary constants. The conditions (2.17) lead to

$$u^{\text{RAB}} = 0, \quad v^{\text{RAB}} = \bar{\psi}r \tag{2.21}$$

Thus, along AB we have

$$u_{|AB}^{\text{RAB}} = 0 \quad v_{|AB}^{\text{RAB}} = \bar{\psi}r_2 \tag{2.22}$$

Let us construct the fields  $u^{\text{NAC}}, v^{\text{NAC}}$  within NAC (Fig. 4).

By (2.22) the fields  $u, v$  within NC must satisfy the following conditions at A:

$$u_A^{\text{NAC}} = \bar{\psi}r_2, \quad v_A^{\text{NAC}} = 0 \tag{2.23}$$

The representation  $(u, v)$  in NAC is of the form (2.20), or

$$\begin{aligned} u^{\text{NAC}}(r, \vartheta) &= C_1 \cos(\vartheta - \varphi), \\ v^{\text{NAC}}(r, \vartheta) &= \psi r - C_1 \sin(\vartheta - \varphi) \end{aligned} \tag{2.24}$$

The conditions (2.22) result in

$$C_1 \cos(\theta_1 - \varphi) = \bar{\psi}r_2 \quad \psi r_1 - C_1 \sin(\theta_1 - \varphi) = 0 \tag{2.25}$$

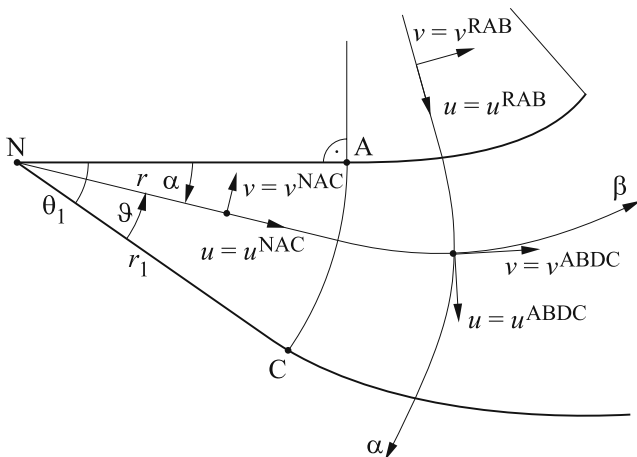


Fig. 4 Polar parameterization of the domain NAC

Let us introduce the constants

$$C_1^0 = C_1 \sin(\theta_1 - \varphi), \quad C_2^0 = -C_1 \cos(\theta_1 - \varphi) \tag{2.26}$$

Hence

$$\bar{\psi}r_2 = -C_2^0, \quad \psi r_1 = C_1^0 \tag{2.27}$$

The representations of  $(u, v)$  are

Domain RAB

$$u = 0, \quad v = -\frac{C_2^0}{r_2}r \tag{2.28}$$

Domain NAC

$$\begin{aligned} u &= C_1^0 \sin \alpha - C_2^0 \cos \alpha, \\ v &= -C_1^0 \left( \cos \alpha - \frac{r}{r_1} \right) - C_2^0 \sin \alpha \end{aligned} \tag{2.29}$$

Along the lines AB, AC, the fields  $(u, v)$  in ABDC must be compatible with (2.28) and (2.29) or

$$\begin{aligned} u_{|AB}^{\text{ABDC}} &= u_{|AB}^{\text{ARB}}, \quad v_{|AB}^{\text{ABDC}} = v_{|AB}^{\text{ARB}} \\ u_{|AC}^{\text{ABDC}} &= -v_{|AC}^{\text{NAC}}, \quad v_{|AC}^{\text{ABDC}} = u_{|AC}^{\text{NAC}} \end{aligned} \tag{2.30}$$

Consequently, the values of  $u^{\text{ABDC}}, v^{\text{ABDC}}$  on the arc AB refer to the line  $\alpha = 0$

$$u^{\text{ABDC}}(0, \beta) = 0, \quad v^{\text{ABDC}}(0, \beta) = -C_2^0 \tag{2.31}$$

while the values of these fields on the arc AC refer to the case of  $\beta = 0$

$$\begin{aligned} u^{\text{ABDC}}(\alpha, 0) &= C_1^0(\cos \alpha - 1) + C_2^0 \sin \alpha \\ v^{\text{ABDC}}(\alpha, 0) &= C_1^0 \sin \alpha - C_2^0 \cos \alpha \end{aligned} \tag{2.32}$$

Let us pass to the construction of the fields  $u = u^{\text{ABDC}}, v = v^{\text{ABDC}}$ .

According to (2.15) these fields satisfy the partial differential equations of the form

$$\frac{\partial^2 u}{\partial \alpha \partial \beta} - u = 0, \quad \frac{\partial^2 v}{\partial \alpha \partial \beta} - v = 0 \tag{2.33}$$

The values of  $u, v$  at an arbitrary point  $(\lambda, \mu)$  of the domain ABDC are given by the Riemann's formula, cf. (17) in Lewiński et al. (1994a)

$$\begin{aligned} u(\lambda, \mu) &= u(0, 0)G_0(\lambda, \mu) \\ &+ \int_0^\lambda G_0(\lambda - \alpha, \mu) \frac{\partial u(\alpha, 0)}{\partial \alpha} d\alpha \\ &+ \int_0^\mu G_0(\lambda, \mu - \beta) \frac{\partial u(0, \beta)}{\partial \beta} d\beta \end{aligned} \tag{2.34}$$

Substitution of (2.31), (2.32) gives

$$u(\lambda, \mu) = -C_1^0 \int_0^\lambda G_0(\lambda - \alpha, \mu) \sin \alpha d\alpha + C_2^0 \int_0^\mu G_0(\lambda - \alpha, \mu) \cos \alpha d\alpha \quad (2.35)$$

By using the formulae (16) of Lewiński et al. (1994a) one finds

$$u(\lambda, \mu) = -C_1^0 F_2(\lambda, \mu) + C_2^0 F_1(\lambda, \mu) \quad (2.36)$$

while applying the differentiation rules (4) of Lewiński et al. (1994a) we arrive at

$$v(\lambda, \mu) = C_1^0 F_1(\lambda, \mu) - C_2^0 F_0(\lambda, \mu) \quad (2.37)$$

Now we can determine the displacements at the node D

$$u(D) = u(\theta_1, \theta_2), \quad v(D) = v(\theta_1, \theta_2) \quad (2.38)$$

The displacements of the point D in the directions  $x$  and  $y$  are computed by the rules

$$w_x(D) = u(D) \cos(\gamma_2 + \phi_D) - v(D) \sin(\gamma_2 + \phi_D),$$

$$w_y(D) = u(D) \sin(\gamma_2 + \phi_D) + v(D) \cos(\gamma_2 + \phi_D) \quad (2.39)$$

where

$$\phi_D = \theta_2 - \theta_1 \quad (2.40)$$

Substitution of (2.36)–(2.38) results in

$$w_x(D) = C_1^0 h_1(\theta_1, \theta_2) + C_2^0 h_2(\theta_1, \theta_2),$$

$$w_y(D) = C_1^0 k_1(\theta_1, \theta_2) + C_2^0 k_2(\theta_1, \theta_2) \quad (2.41)$$

where  $h_1, h_2, k_1, k_2$  are given by the (2.10) and (2.11).

We shall find the displacements of the node N in the directions  $x$  and  $y$ . First we shall compute the displacements in the polar coordinate system within ANC. Substitution of  $r = 0, \alpha = 0$  in (2.29) gives

$$u^{NAC}(N) = -C_2^0, \quad v^{NAC}(N) = -C_1^0 \quad (2.42)$$

Thus, see Fig. 5

$$w_x(N) = -u^{NAC}(N) \cos \gamma_1 - v^{NAC}(N) \sin \gamma_1$$

$$w_y(N) = u^{NAC}(N) \sin \gamma_1 - v^{NAC}(N) \cos \gamma_1 \quad (2.43)$$

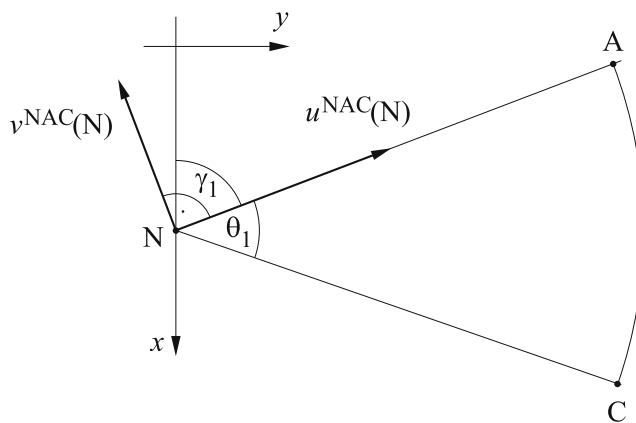


Fig. 5 Displacements  $u^{NAC}(N), v^{NAC}(N)$

Substitution of (2.42) gives

$$w_x(N) = C_2^0 \cos \gamma_1 + C_1^0 \sin \gamma_1$$

$$w_y(N) = -C_2^0 \sin \gamma_1 + C_1^0 \cos \gamma_1 \quad (2.44)$$

Now we are prepared to applying the variational equation (2.14). The displacements fields ( $u, v$ ) assumed are chosen such that the left hand side of (2.14) vanishes, or  $\mathcal{L}(u, v) = 0$ , where  $\mathcal{L}$  represents the virtual work of all loads. Since the fields  $u$  and  $v$  vanish at R, the virtual work is done by the other point loads

$$F_x w_x(D) + F_y w_y(D) + Q_x w_x(N) + Q_y w_y(N) = 0 \quad (2.45)$$

where  $w_x(D), w_y(D), w_x(N), w_y(N)$  are given by (2.41) and (2.44) depending on two parameters  $C_1^0$  and  $C_2^0$ . Since  $Q_y$  can be computed by using (2.12) we shall isolate the formula which determines  $Q_x$ . To this end we choose

$$C_1^0 = C_2^0 \tan \gamma_1 \quad (2.46)$$

to make  $w_y(N)$  zero. Substitution (2.46) into (2.41), (2.44) and (2.45) gives the formula we have looked for

$$Q_x = -[\sin \gamma_1 h_1(\theta_1, \theta_2) + \cos \gamma_1 h_2(\theta_1, \theta_2)] F_x - [\sin \gamma_1 k_1(\theta_1, \theta_2) + \cos \gamma_1 k_2(\theta_1, \theta_2)] F_y \quad (2.47)$$

Let us stress once again that this formula was originally found by Chan (1966).

#### 2.4 The volume of the optimal framework

The volume of the framework of Fig. 2 will be found by the kinematic method. We shall construct a virtual field of displacements ( $u, v$ ) satisfying the Michell conditions

$$\varepsilon_I = 1, \quad \varepsilon_{II} = -1 \quad (2.48)$$

within the whole feasible domain, being the half-plane  $y \geq 0$ . Then we shall determine the volume of the lightest framework by the known rule

$$V = \frac{1}{\sigma_p} \mathcal{L}(u, v) \tag{2.49}$$

where  $\mathcal{L}$  represents the work of the given loads on the given field  $(u, v)$ . We shall assume that the components  $(u, v)$  vanish at R; then  $\mathcal{L}$  becomes the virtual work of the forces  $Q_x, Q_y, F_x, F_y$ .

The construction of the virtual fields  $(u, v)$  starts with the triangular domain RAN, parameterized by the Cartesian system  $(x_0, y_0)$ , see Fig. 6.

Let us assume that the bar RB is in tension. Then the fields  $(u, v)$  satisfying (2.48) and vanishing at R are of the form

$$\begin{aligned} u^{\text{RAN}} &= x_0 - C y_0 + r_2, \\ v^{\text{RAN}} &= -y_0 + C x_0 + C r_2 \end{aligned} \tag{2.50}$$

where  $C$  is a constant. Let us consider the domain RBA with the polar parameterization  $(r, \vartheta)$ , see Fig. 7.

According to (77) in Lewiński and Rozvany (2007) we have

$$u^{\text{RBA}} = r, \quad v^{\text{RBA}} = -2r\vartheta + \psi r \tag{2.51}$$

since the bar RB is in tension while point R does not move. The fields (2.50) and (2.51) must be compatible, i.e. the continuity conditions along RA should hold. This links two constants:

$$C = \psi \tag{2.52}$$

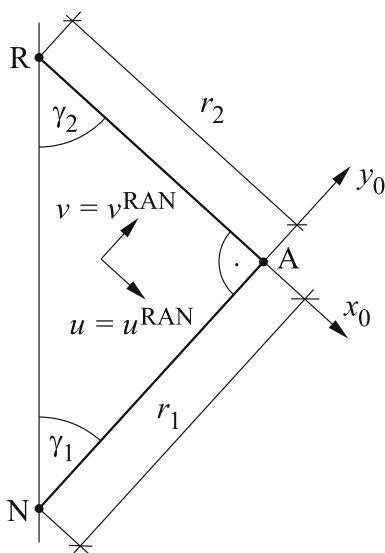


Fig. 6 Parameterization of the triangle RAN

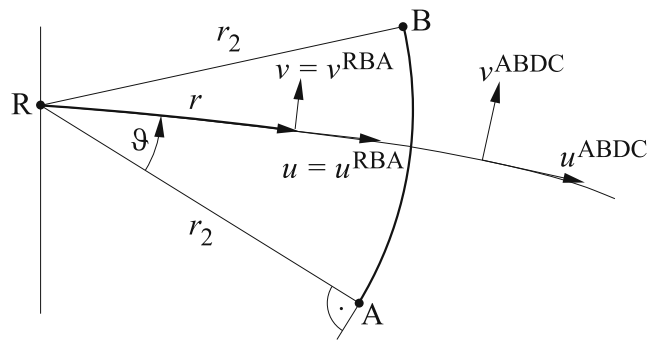


Fig. 7 The domain RBA. Polar parameterization

Consider the domain NAC. We assume that the radial fibres are in compression. Thus, according to (77) in Lewiński and Rozvany (2007) we have

$$\begin{aligned} u^{\text{NAC}} &= -r + C_1 \cos(\vartheta - \varphi), \\ v^{\text{NAC}} &= 2r\vartheta + \tilde{\psi}r - C_1 \sin(\vartheta - \varphi) \end{aligned} \tag{2.53}$$

The compatibility conditions linking the fields (2.50) and (2.53) along NA result in the conditions

$$\begin{aligned} \tilde{\psi} &= \psi - 2\theta_1 \\ C_1 \cos(\theta_1 - \varphi) &= \psi r_2 + r_1 \\ C_1 \sin(\theta_1 - \varphi) &= \psi r_1 + r_2 \end{aligned} \tag{2.54}$$

Substitution of (2.54) into (2.53), along with the formula  $\vartheta = \theta_1 - \alpha$  results in

$$\begin{aligned} u^{\text{NAC}} &= -r + (\psi r_2 + r_1) \cos \alpha + (\psi r_1 + r_2) \sin \alpha \\ v^{\text{NAC}} &= -2r\alpha + \psi r - (\psi r_1 + r_2) \cos \alpha \\ &\quad + (\psi r_2 + r_1) \sin \alpha \end{aligned} \tag{2.55}$$

The components of displacements of node N (Fig. 8), defined as in domain RAN, are given by

$$u^{\text{RAN}}(N) = \psi r_1 + r_2, \quad v^{\text{RAN}}(N) = r_1 + \psi r_2 \tag{2.56}$$

where we have made use of:  $x_0 = 0, y_0 = -r_1, C = \psi$ .

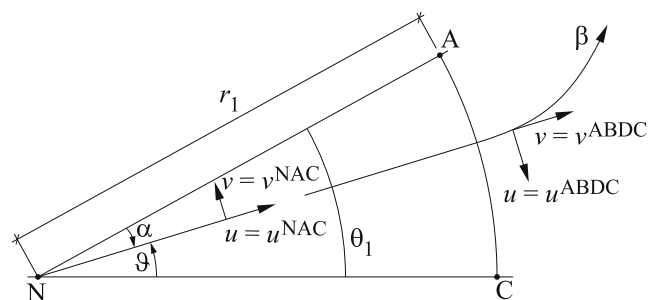


Fig. 8 Polar parameterization of the domain NAC

The displacements of N in the directions  $x$  and  $y$  are

$$\begin{aligned} w_x(N) &= u^{\text{RAN}}(N) \sin \gamma_1 - v^{\text{RAN}}(N) \cos \gamma_1 \\ w_y(N) &= u^{\text{RAN}}(N) \cos \gamma_1 + v^{\text{RAN}}(N) \sin \gamma_1 \end{aligned} \tag{2.57}$$

or

$$\begin{aligned} w_x(N) &= \frac{1}{d} [(r_2)^2 - (r_1)^2] \\ w_y(N) &= \frac{1}{d} [\psi((r_1)^2 + (r_2)^2) + 2r_1r_2] \end{aligned} \tag{2.58}$$

We see now that constant  $\psi$  represents a small angle of rigid rotation of the whole structure around point R.

Let us pass now to the construction of displacements  $(u, v)$  in the domain ABDC, referred to the lines  $\alpha$  and  $\beta$ . One should determine the values of these fields along the arcs AB and AC. Due to continuity of displacements on AB we observe that

$$\begin{aligned} u^{\text{ABDC}}(\alpha = 0, \beta) &= u^{\text{RBA}}(r = r_2, \vartheta = \beta) \\ v^{\text{ABDC}}(\alpha = 0, \beta) &= v^{\text{RBA}}(r = r_2, \vartheta = \beta) \end{aligned} \tag{2.59}$$

or

$$\begin{aligned} u^{\text{ABDC}}(0, \beta) &= r_2 \\ v^{\text{ABDC}}(0, \beta) &= -2r_2\beta + \psi r_2 \end{aligned} \tag{2.60}$$

By continuity conditions along AC we have

$$\begin{aligned} u^{\text{ABDC}}(\alpha, \beta = 0) &= -v^{\text{NAC}}(r = r_1, \alpha) \\ v^{\text{ABDC}}(\alpha, \beta = 0) &= u^{\text{NAC}}(r = r_1, \alpha) \end{aligned} \tag{2.61}$$

hence

$$\begin{aligned} u^{\text{ABDC}}(\alpha, 0) &= 2r_1\alpha - \psi r_1 + (\psi r_1 + r_2) \cos \alpha \\ &\quad - (\psi r_2 + r_1) \sin \alpha \\ v^{\text{ABDC}}(\alpha, 0) &= -r_1 + (\psi r_2 + r_1) \cos \alpha \\ &\quad + (\psi r_1 + r_2) \sin \alpha \end{aligned} \tag{2.62}$$

The quantity  $\psi$  is arbitrary, since it represents an angle of rigid body rotation around R. Let us assume this constant such that  $\psi r_1 + r_2 = -(\psi r_2 + r_1)$ . Then  $\psi = -1$ .

Let us introduce the auxiliary field within ABDC

$$u^0(\alpha, \beta) = u(\alpha, \beta) - 2\alpha A(\alpha, \beta) \tag{2.63}$$

see (66) in Lewiński et al. (1994a). We compute the values of the Lamé coefficient  $A$  along AB and AC

$$\begin{aligned} A(0, \beta) &= r_1 G_0(0, \beta) + r_2 G_1(\beta, 0) = r_1 + \beta r_2 \\ A(\alpha, 0) &= r_1 G_0(\alpha, 0) + r_2 G_1(0, \alpha) = r_1 \end{aligned} \tag{2.64}$$

as well as the field  $u = u^{\text{ABDC}}$

$$\begin{aligned} u(0, \beta) &= r_2 \\ u(\alpha, 0) &= 2r_1\alpha + r_1 + (r_2 - r_1)(\cos \alpha + \sin \alpha) \end{aligned} \tag{2.65}$$

The values of the field  $u^0$  on AB and AC are

$$\begin{aligned} u^0(0, \beta) &= r_2 \\ u^0(\alpha, 0) &= r_1 + (r_2 - r_1)(\cos \alpha + \sin \alpha) \end{aligned} \tag{2.66}$$

The field  $u^0$  satisfies (2.33). Its solution has the form (2.34). We compute the derivatives

$$\begin{aligned} \frac{\partial u^0(\alpha, 0)}{\partial \alpha} &= (r_2 - r_1)(\cos \alpha - \sin \alpha) \\ \frac{\partial u^0(0, \beta)}{\partial \beta} &= 0, \quad u^0(0, 0) = r_2 \end{aligned} \tag{2.67}$$

Substitution of these results into (2.34) gives

$$\begin{aligned} u^0(\lambda, \mu) &= r_2 G_0(\lambda, \mu) \\ &\quad + (r_2 - r_1) \int_0^\lambda G_0(\lambda - \alpha, \mu) \cos \alpha d\alpha \\ &\quad - (r_2 - r_1) \int_0^\lambda G_0(\lambda - \alpha, \mu) \sin \alpha d\alpha \end{aligned} \tag{2.68}$$

By using the formulae (16) of Lewiński et al. (1994a) one finds

$$\begin{aligned} u^0(\lambda, \mu) &= r_2 G_0(\lambda, \mu) + (r_2 - r_1) \\ &\quad \times [F_1(\lambda, \mu) - F_2(\lambda, \mu)] \end{aligned} \tag{2.69}$$

and then we find  $u(\lambda, \mu)$  by (2.63) and (2.4); the result reads

$$\begin{aligned} u(\lambda, \mu) &= 2r_1\lambda G_0(\lambda, \mu) \\ &\quad + r_2 [G_0(\lambda, \mu) + 2\mu G_1(\lambda, \mu)] \\ &\quad + (r_2 - r_1) [F_1(\lambda, \mu) - F_2(\lambda, \mu)] \end{aligned} \tag{2.70}$$

The field  $v$  is found from the equation

$$v(\lambda, \mu) = A(\lambda, \mu) - \frac{\partial u(\lambda, \mu)}{\partial \lambda} \tag{2.71}$$

see (65) in Lewiński et al. (1994a). By using the differentiation rules (4) of the latter paper one finds

$$\begin{aligned} v(\lambda, \mu) &= -2r_1\mu G_1(\lambda, \mu) \\ &\quad - r_2(1 + 2\mu)G_0(\lambda, \mu) \\ &\quad + (r_2 - r_1) [F_1(\lambda, \mu) + F_2(\lambda, \mu)] \end{aligned} \tag{2.72}$$



The displacements  $w_x(D)$ ,  $w_y(D)$  of point D of coordinates  $(\theta_1, \theta_2)$  are determined by (2.39), where

$$u(D) = u(\theta_1, \theta_2), \quad v(D) = v(\theta_1, \theta_2) \tag{2.73}$$

The displacements  $w_x(N)$ ,  $w_y(N)$  of point N are given by (2.58), where  $\psi = -1$ . Having found the displacements of the nodes N and D as well as the values of the forces  $Q_x$  and  $Q_y$  given by (2.12) and (2.47), one can compute the volume of the whole framework by using (2.49), or

$$V = \frac{1}{\sigma_p} [F_x w_x(D) + F_y w_y(D) + Q_x w_x(N) + Q_y w_y(N)] \tag{2.74}$$

Let us emphasize once again that the result above is not valid in general; it refers to the case of such inclination of the force  $F = (F_x, F_y)$  that the bar RBD is in tension and the bar NCD is in compression. The resultant  $F$  must lie between the lines  $l_1$  and  $l_2$  shown in Fig. 2.

### 3 Theorem of Henry Chan

Assume that

$$F_y = 0, \quad \theta_1 = \theta_2 \tag{3.1}$$

Then the reactions  $P$  and  $Q$ —equilibrating the optimal framework—intersect at point D, see Fig. 9. This property was noted and proved by Chan (1966).

Because the report: Chan (1966) is unavailable it is thought appropriate to show here the proof of this statement. It is sufficient to prove that (3.1) implies the equality

$$\frac{x_D - d}{y_D} = \frac{Q_x}{Q_y} \tag{3.2}$$

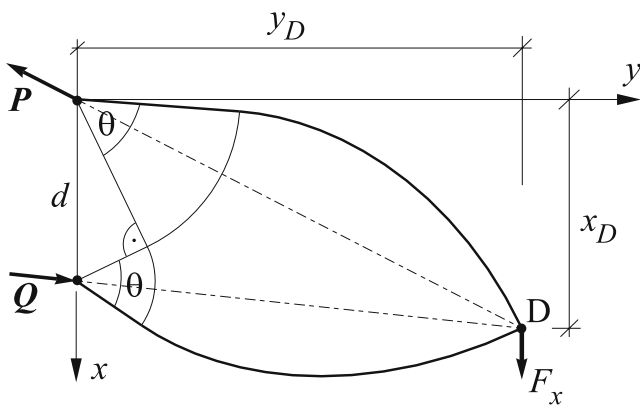


Fig. 9 Illustration of the theorem by H.S.Y. Chan

for the case of  $y_D \neq 0$ ,  $Q_y \neq 0$ . Indeed, the equality (2.12) along with  $F_y = 0$  gives

$$Q_y = \frac{y_D}{d} F_x \tag{3.3}$$

while (2.47) gives

$$Q_x = -[\sin \gamma_1 h_1(\theta, \theta) + \cos \gamma_1 h_2(\theta, \theta)] F_x \tag{3.4}$$

where  $\theta_1 = \theta_2 = \theta$ . The (3.3) and (3.4) imply

$$y_D \frac{Q_x}{Q_y} = -d [\sin \gamma_1 h_1(\theta, \theta) + \cos \gamma_1 h_2(\theta, \theta)] \tag{3.5}$$

and then

$$y_D \frac{Q_x}{Q_y} = d [\cos^2 \gamma_2 F_2(\theta, \theta) - \sin^2 \gamma_2 F_0(\theta, \theta)] \tag{3.6}$$

According to (2.9) we have  $x(\theta, \theta) = x_D$  or

$$x_D = d [\sin \gamma_2 k_1(\theta, \theta) - \cos \gamma_2 k_2(\theta, \theta)] \tag{3.7}$$

Substitution of (2.11) gives

$$x_D - d = d [\cos^2 \gamma_2 F_2(\theta, \theta) - \sin^2 \gamma_2 F_0(\theta, \theta)] \tag{3.8}$$

which ends the proof of the theorem. We have made use of the identity

$$F_0(\theta, \theta) - F_2(\theta, \theta) = 1 \tag{3.9}$$

see Lewiński et al. (1994a), (7)–(12).

### 4 Exemplary optimal frameworks equilibrating systems of three forces

#### 4.1 The frameworks illustrating the theorem by Henry Chan

Let us assume that the following quantities are given

$$\sigma_p, F_x = 1, F_y = 0, \quad d, \gamma_1, \theta_1 = \theta_2 = \theta$$

First the following quantities are computed

$$\xi_D = 2 \frac{x_D}{d}, \quad \eta_D = 2 \frac{y_D}{d} \tag{4.1}$$

by using (2.9). These equations can be re-written as follows

$$\begin{aligned} \xi_D &= 1 + \cos(2\gamma_2) G_0(\theta, \theta) \\ \eta_D &= 2F_1(\theta, \theta) + \sin(2\gamma_2) G_0(\theta, \theta) \end{aligned} \tag{4.2}$$

where  $\gamma_2 = \frac{\pi}{2} - \gamma_1$ . We have made use of the identity

$$F_0(\theta, \theta) + F_2(\theta, \theta) = G_0(\theta, \theta) \tag{4.3}$$

Having  $x_D, y_D$  we compute  $Q_y$  by (3.3) and  $Q_x$  by (3.2). The volume of the optimal structure is computed by using (2.74) and referred to  $U_0 = \frac{F_x d}{\sigma_p}$ .

Four examples satisfying (3.1) will be dealt with. In the first case  $\gamma_2 = 45^\circ$  and  $\theta = 50^\circ$ , which results in the symmetric framework, cf. Fig. 10. In the second case of  $\gamma_2 = 60^\circ$  and  $\theta = 30^\circ$  the external cable of the upper fan is exactly horizontal, see Fig. 11.

To enrich the discussion, let us now assume that the point D is known and the following quantities are given

$$\sigma_p, F_x = 1, F_y = 0, \quad d, x_D, y_D$$

Then  $\gamma_2$  and  $\theta$  can be found from the set of (4.2).

This problem is harder than before because the equations are transcendental. Solutions can only be obtained numerically in general. Nevertheless, it is not difficult to calculate  $\gamma_2$  and  $\theta$  for reasonably assumed  $x_D$  and  $y_D$ . For instance the Figs. 12 and 13 present two distinctive examples for differently assumed positions of point D.

#### 4.2 Other exemplary solutions

The four examples presented in Figs. 10–13 relate to the particular case (3.1) studied by Chan (1966), for angles  $\theta_1$  and  $\theta_2$  in both fans being equal. Obviously, the formulas given in Section 2 are more general (neither  $\theta_1 = \theta_2$  nor  $F_y = 0$ ). They enable constructing other optimal frameworks equilibrating systems of three forces, not necessarily crossing point D. It is possible to investigate many cases with differently chosen sets of known parameters. However, from practical point of view the most interesting is the problem for given three forces  $F, Q, P$  applied at points D, N, R. Without losing generality one can assume that

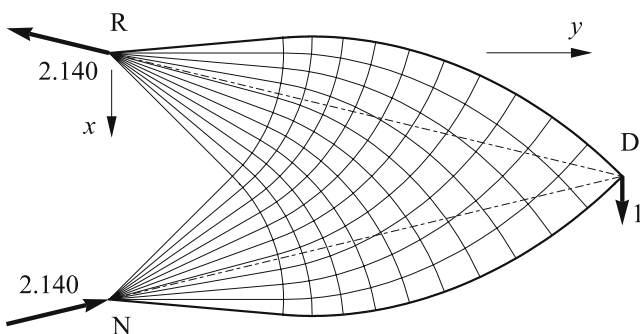


**Fig. 10** Optimal framework for given  $\gamma_2 = 45^\circ$  and  $\theta = 50^\circ$ . The volume:  $V = 7.451U_0$ . Here  $x_D = 0.5d, y_D = 2.081d$

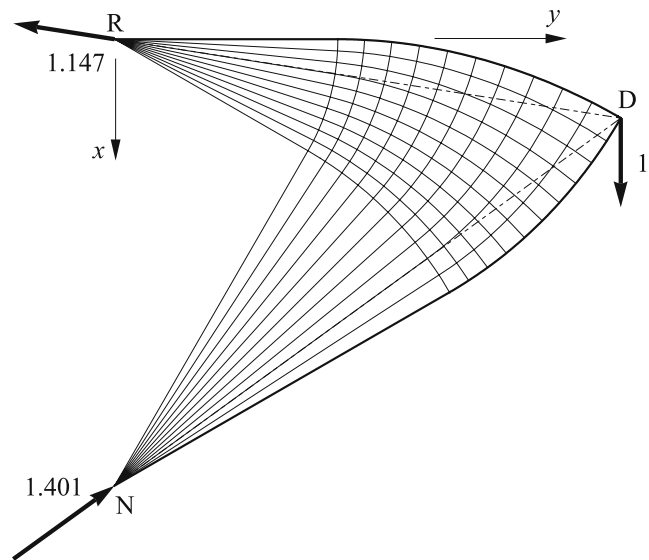


**Fig. 11** Optimal framework for given  $\gamma_2 = 60^\circ$  and  $\theta = 30^\circ$ . The volume:  $V = 3.094U_0$ . Here  $x_D = 0.1766d, y_D = 1.134d$

point R lies at the origin of the  $(x, y)$  system and point N lies on the  $x$  axis (see Fig. 2). As before point D is determined by its coordinates  $x_D, y_D$ . Note that structure under consideration is not supported at any node, hence the system of three forces has to be self-equilibrated. It means that only three of six components of loads:  $F_x, F_y, Q_x, Q_y, P_x, P_y$ , can be chosen independently because they have to satisfy three equilibrium equations:

$$\begin{aligned} P_x + Q_x + F_x &= 0 \\ P_y + Q_y + F_y &= 0 \\ Q_y d + F_y x_D - F_x y_D &= 0 \end{aligned} \tag{4.4}$$

Let us assume that  $F_x, F_y, Q_x$  will be chosen as the independent parameters and the remaining quantities  $Q_y, P_x, P_y$

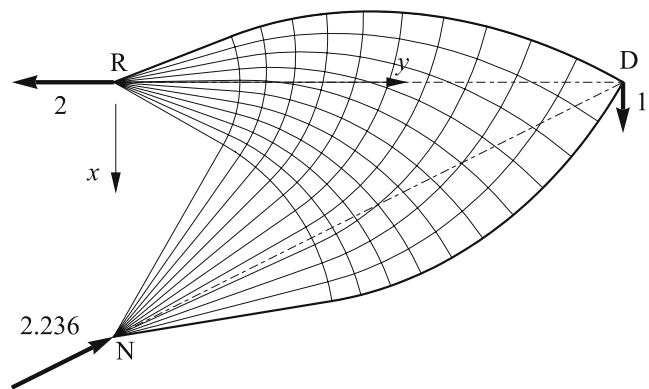


**Fig. 12** Optimal framework for given  $x_D = 0$  and  $y_D = 2$ . The volume:  $V = 7.273U_0$ . Here  $\gamma_2 = 60.31^\circ, \theta = 51.00^\circ$

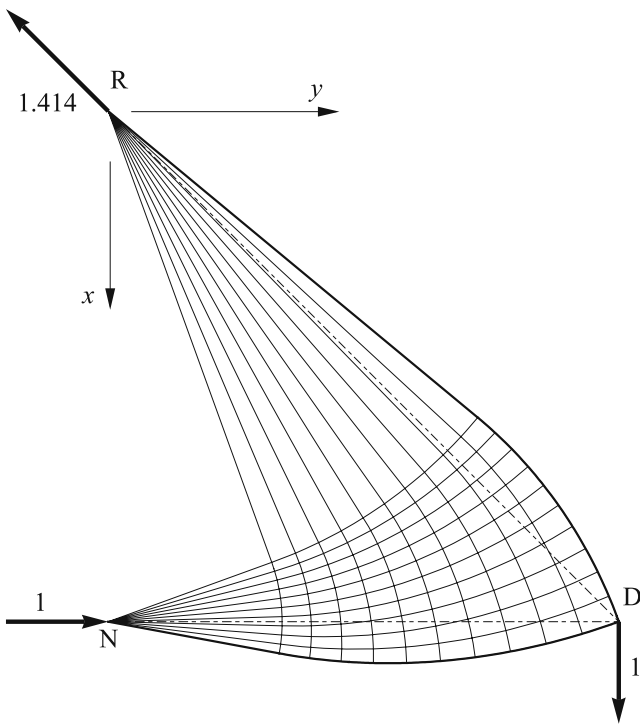


**Fig. 13** Optimal framework for given  $x_D = d, y_D = d$ . The volume:  $V = 2.835U_0$ . Here  $\gamma_2 = 19.92^\circ, \theta = 30.42^\circ$

will be determined from (4.4). Thus in the present problem the following quantities are given:

$$\sigma_p, d, x_D, y_D, F_x, F_y, Q_x \tag{4.5}$$

It should be understood that these quantities may not be fully free if we want to solve the problem using the formulas

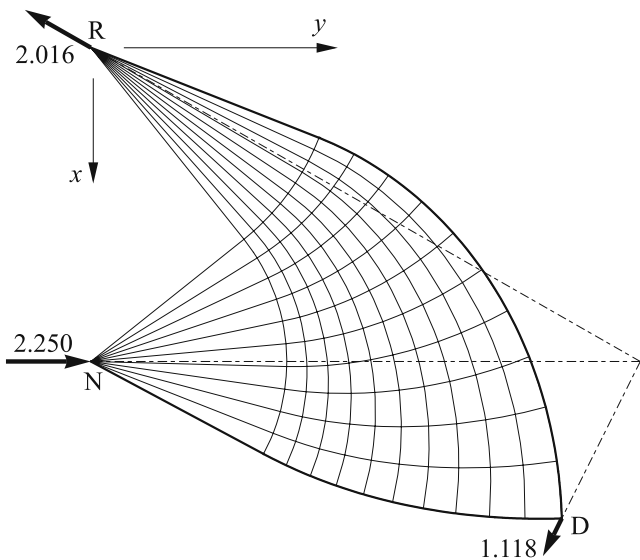


**Fig. 14** Optimal framework for  $x_D = 1.5d, y_D = 1.5d, F_x = 1, F_y = -0.5, Q_x = 0$ . The volume:  $V = 6.831U_0$ . Here  $\theta_1 = 66.77^\circ, \theta_2 = 29.81^\circ, \gamma_2 = 38.61^\circ$

derived in Section 2; they have a wide but restricted range of application (they are not universal). For example, the direction of the resultant force  $F$  should lie in the marked regions around the point D (see Fig. 2), which however is not known in advance. Therefore, the results obtained from these formulas have to be carefully verified after finding the solution. It means that the general problem of three forces is still the challenge.

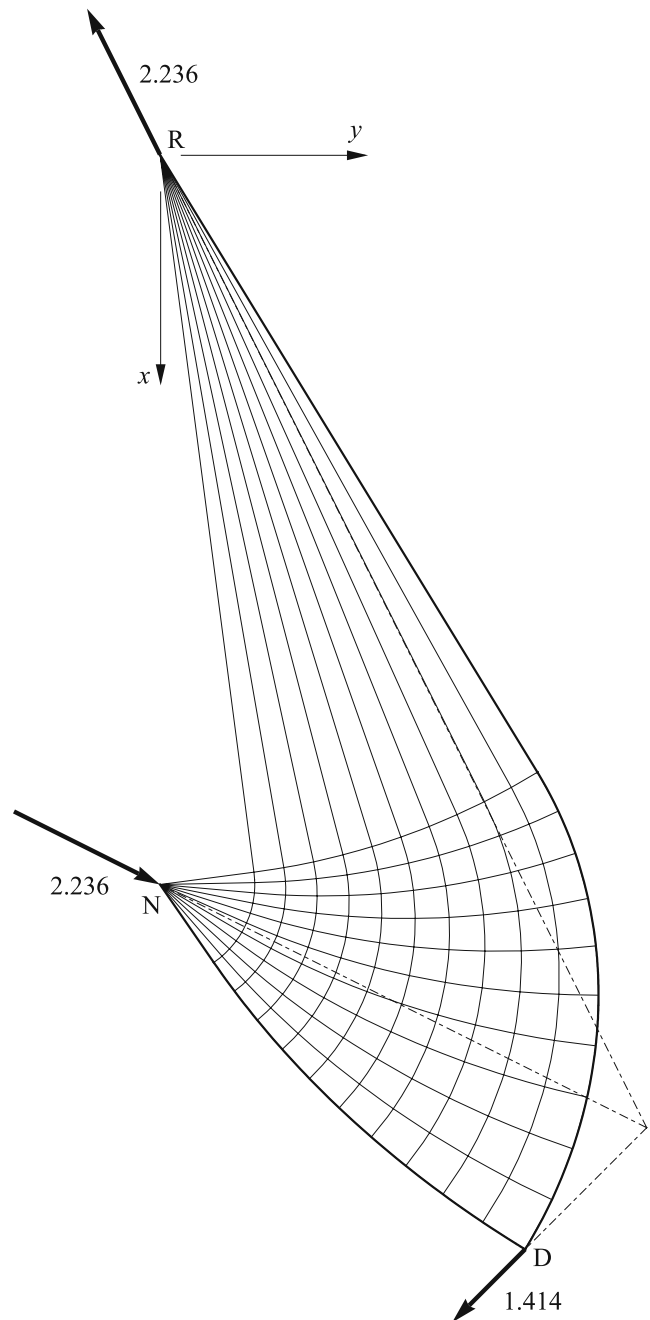


**Fig. 15** Optimal framework for  $x_D = 1.5d, y_D = 0.5d, F_x = 1, F_y = -1, Q_x = 1$ . The volume  $V = 4.750U_0$ . Here  $\theta_1 = 62.89^\circ, \theta_2 = 23.96^\circ, \gamma_2 = 7.453^\circ$

The geometry of the optimal layout is defined by three angles:  $\theta_1, \theta_2, \gamma_2$  which are governed by three equations (followed from (2.9)–(2.11) and (2.47)):

$$\begin{aligned} x_D &= d[\sin \gamma_2 k_1(\theta_1, \theta_2) - \cos \gamma_2 k_2(\theta_1, \theta_2)] \\ y_D &= d[-\sin \gamma_2 h_1(\theta_1, \theta_2) + \cos \gamma_2 h_2(\theta_1, \theta_2)] \\ Q_x &= -F_x[\cos \gamma_2 h_1(\theta_1, \theta_2) + \sin \gamma_2 h_2(\theta_1, \theta_2)] \\ &\quad - F_y[\cos \gamma_2 k_1(\theta_1, \theta_2) + \sin \gamma_2 k_2(\theta_1, \theta_2)] \end{aligned} \quad (4.6)$$

As before the system of equations is transcendental and the solution can only be obtained in a numerical way. It is however worthy of note that the unique solution can be found for a very wide range of input data. The problem of uniqueness of the solution is not the topic of this paper and will not be dealt with here.

Two pin-jointed frames shown in Figs. 14 and 15 are representative examples of the optimal structures found by solving the system (4.6). The first example was calculated for  $x_D = 1.5d, y_D = 1.5d, F_x = 1, F_y = -0.5, Q_x = 0$ . The remaining three forces are defined by (4.4) and equal to  $Q_y = 2.25, P_x = -1, P_y = -1.75$ . The optimal layout with the resultant forces at the nodes R, D, N is shown in Fig. 14. The second example shown in Fig. 15 was calculated for  $x_D = 1.5d, y_D = 0.5d, F_x = 1, F_y = -1, Q_x = 1$ . The remaining forces are equal to  $Q_y = 2, P_x = -2, P_y = -1$ . The angle  $\gamma_2 = 7.453^\circ$ ; it is small value so the radii  $r_1$  and  $r_2$  of the two fans are very distinct. Note that in both examples the directions of the resultant force  $F$  are admissible, hence the presented results are correct.

**5 The lightest fully stressed pin-jointed frameworks transmitting two vertical forces to two fixed supports**

**5.1 Prediction of the optimal solution**

The analytical solution of the three forces problem can be used to construct the optimal frameworks transmitting two vertical forces of magnitude  $P$  to two fixed supports R and R', see Fig. 16. We note that the forces applied are symmetric with respect to the supporting nodes R and R'.

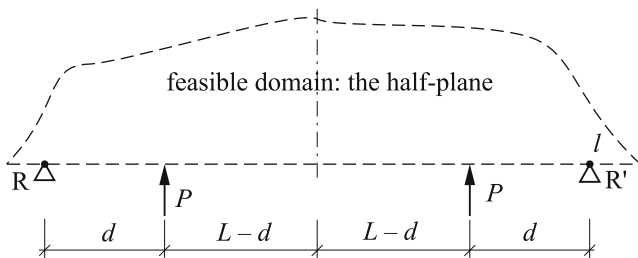


Fig. 16 Problem formulation

The feasible domain is the half plane over the line  $l$  linking R and R'. Therefore, given are

$\sigma_p, d, P, L,$

where  $2L = |RR'|$ , see Fig. 16. Let us introduce a non-dimensional parameter  $\xi = d/L$  describing the positions of applied loads and the referential volume  $V_0 = PL/\sigma_p$ . The main unknowns are the characteristic dimensions of the optimum structure and its volume. The first numerical predictions of the problem considered were found in the paper by McConnel (1974), while the first correct topology of the

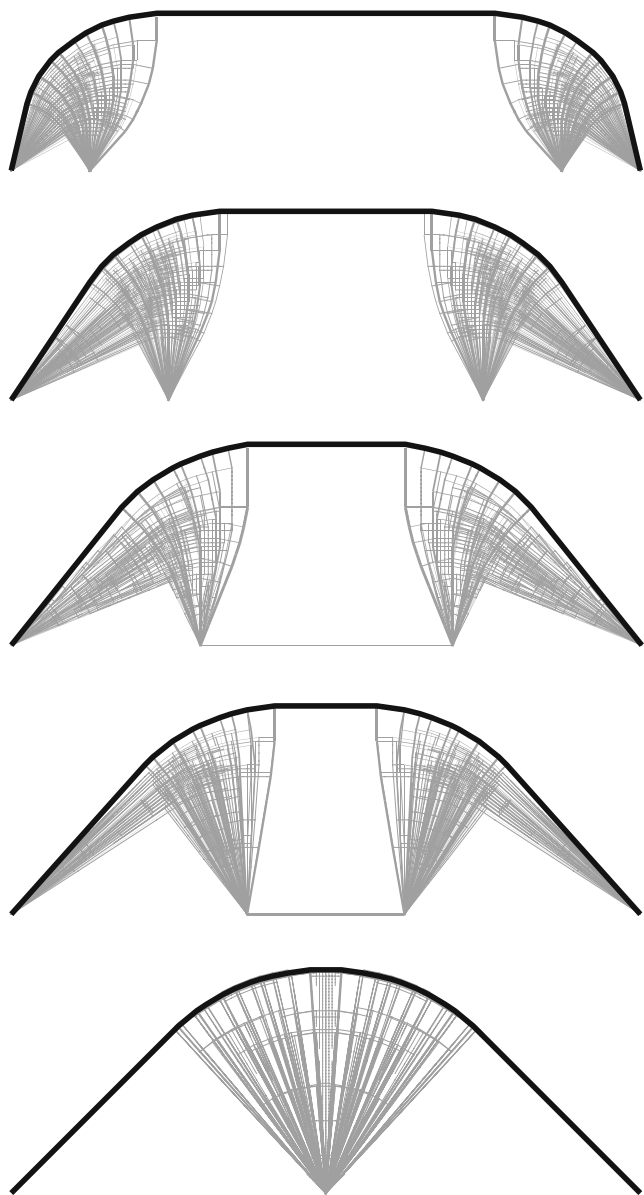
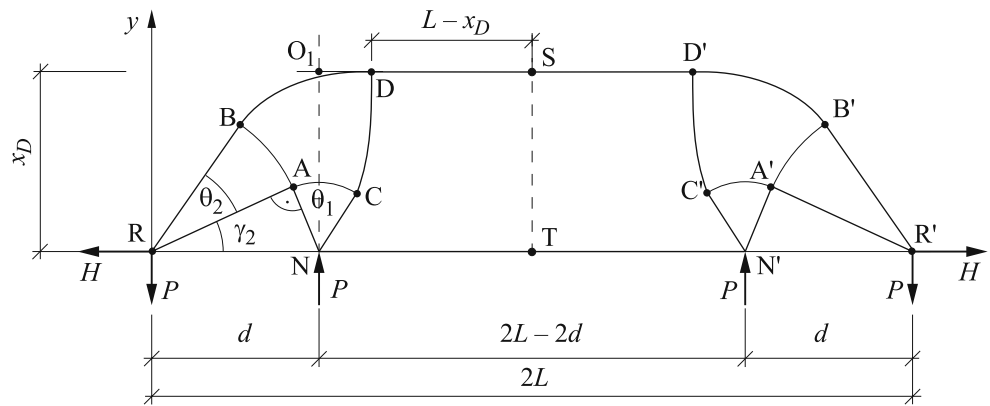


Fig. 17 Selected numerical solutions for  $\xi = 0.25, 0.5, 0.6, 0.75$  and 1

**Fig. 18** The layout of the solution



analytical solution for the problem considered has been suggested intuitively by G.I.N. Rozvany (see Lógó et al. 2009). The latter results, along with new numerical results by Sokół (2010) shown in Fig. 17 have been an inspiration for the present authors to predict the exact layouts of the analytical solutions.

The solutions presented in Fig. 17 suggest that the optimal framework consists of two frameworks constructed in Sections 2–4 of the present paper and of one or two horizontal bars DD' and NN', cf. Fig. 18. More detailed numerical tests showed that the bottom bar NN' appears only for  $\xi \geq 0.6$ . Of course the precision of this prediction is limited due to discretization error of possible to apply density of ground structure. It will be improved by the analytical method presented below. We shall separately investigate two cases: with and without the bottom horizontal bar NN'. Moreover, it should be emphasized that geometry of the optimal structure for fixed  $\xi$  is fully determined by three angles  $\theta_1$ ,  $\theta_2$ , and  $\gamma_2$ . Other geometrical quantities, like coordinates  $x_D$ ,  $y_D$ , lengths of bars DD' and NN', etc., are directly dependent on these three angular parameters.

The layout of the envisaged optimal solution is outlined in Fig. 18. Thus we expect that the curved bar RBDD'B'R' which reinforces the structure from the upper side is of constant and finite area of the cross sections. One family of the fibers of the domain ABDC touches this bar orthogonally transmitting no tangent tractions. Consequently, the axial stress resultant in RB within this bar is constant along the boundary BD. The bar RB is also not subjected to tangent forces, hence the axial stress resultant in RB is constant. The reaction at R of components  $H$  and  $P$  is directed towards point  $O_1$ . We know from the theorem by Chan that  $O_1 = D$  only if  $\theta_1 = \theta_2$ , which is a rare case. The problem of Fig. 18 differs from problems of Figs. 1 and 2 considerably. In the problem of Fig. 18 the force  $Q_y$  is given and equal  $P$ . Let  $N$  be the axial force in member DD'. Then  $F_x = N$  and  $F_y = 0$ . Thus the tangent line to the curve  $\beta = \theta_2$  (or to the line RBD) at  $D = D(\theta_1, \theta_2)$  is par-

allel to the  $x$  axis. Since this tangent line makes an angle  $\phi_D = \phi(\theta_1, \theta_2) = \theta_2 - \theta_1$  with the axis  $x_0$ , hence

$$\gamma_2 + \theta_2 - \theta_1 = 0 \tag{5.1}$$

or  $\theta_1 = \gamma_2 + \theta_2$ . This formula eliminates one of three main unknowns and is valid for both cases under consideration.

### 5.2 Case 1: the optimal framework without the bottom bar NN'

Let us now investigate the first case for the structure without the bottom bar NN', see Fig. 19. The problem is very specific because  $Q_x = 0$  and  $F_y = 0$  simultaneously. By (2.47), with using (5.1) one arrives at

$$\sin \gamma_1 h_1(\theta_2 + \gamma_2, \theta_2) + \cos \gamma_1 h_2(\theta_2 + \gamma_2, \theta_2) = 0. \tag{5.2}$$

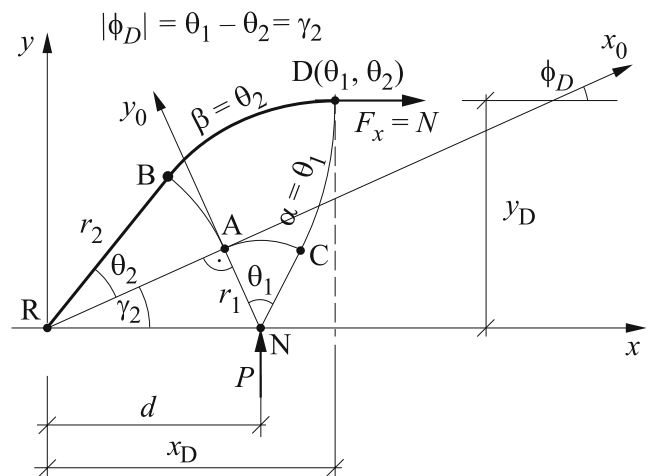


**Fig. 19** The three forces problem with the force at D being horizontal and the force at N being vertical

By (2.10) we compute

$$\begin{aligned} h_1(\theta_2 + \gamma_2, \theta_2) &= -F_2(\gamma_2 + \theta_2, \theta_2) \\ h_2(\theta_2 + \gamma_2, \theta_2) &= F_1(\gamma_2 + \theta_2, \theta_2) \end{aligned} \tag{5.3}$$

The (5.2) will be written in the form

$$z(\theta_2, \gamma_2) = 0 \tag{5.4}$$

with

$$\begin{aligned} z(\theta_2, \gamma_2) &= -\cos \gamma_2 F_2(\gamma_2 + \theta_2, \theta_2) \\ &\quad + \sin \gamma_2 F_1(\gamma_2 + \theta_2, \theta_2) \end{aligned} \tag{5.5}$$

Equation (5.4) is transcendental but formally enables one to eliminate the next unknown. More detailed analysis shows that for wide range of possible angles the best control parameter is  $\theta_2$  (it is more convenient than  $\gamma_2$ , which should be treated as the implicit function  $\gamma_2(\theta_2)$ ).

Let us fix  $\theta_2$  for the moment. The value of  $\gamma_2$  is determined by (5.4), then the value of  $\theta_1$  is determined by (5.1). Now we are able to compute all remaining geometrical and mechanical quantities needed for analysis using the formulas derived in Sections 2 and 3. The point  $(x_D, y_D)$  is determined by (2.9)–(2.11). The displacements of points N and D are given by (2.58) and (2.73), respectively. Then we can compute the value of the force  $F_x$  from (3.3), where  $Q_y = P$  is the known (applied) load. We compute the volume  $V_1$  of the structure RBDCNAR by (2.74), assuming  $Q_x = 0$  and  $F_y = 0$ . The volume of the bar DS equals

$$V_2 = \frac{F_x}{\sigma_p} (L - x_D) \tag{5.6}$$

Finally, the total volume  $2\bar{V} = 2V_1 + 2V_2$  of the structure of Fig. 18 (for the present case: without the bottom bar NN') may be written in the form

$$2\bar{V} = 2V_0 \left( \xi \frac{L - x_D + w_x(D)}{y_D} + \frac{w_y(N)}{L} \right) \tag{5.7}$$

This volume should be viewed as a function of two variables  $\theta_2$  and  $\gamma_2$ . We shall choose these variables such that:  $\gamma_2 \in [0, \frac{\pi}{2}]$ ,  $\theta_2 \in [0, \pi]$  to make the volume  $\bar{V}$  as small as possible yet obeying the condition (5.4). This optimization problem may be written as:

$$\min \left\{ \bar{V}(\theta_2, \gamma_2) \mid z(\theta_2, \gamma_2) = 0, \gamma_2 \in \left[ 0, \frac{\pi}{2} \right] \right\} \tag{5.8}$$

The solution to (5.8) may be achieved in many different ways, for example by: (a) using of suitable minimization procedure (numerical approach), (b) converting the problem to one variable  $\theta_2$ , treating  $\bar{V}$  as  $\bar{V}(\theta_2, \gamma_2(\theta_2))$ . The following differentiation rule applies

$$\frac{d\bar{V}}{d\theta_2} = \frac{\partial \bar{V}}{\partial \theta_2} - \frac{\partial \bar{V}}{\partial \gamma_2} \frac{\partial z}{\partial \theta_2} \left( \frac{\partial z}{\partial \gamma_2} \right)^{-1} \tag{5.9}$$

according to the implicit function theorem, or (c) direct involving of Karush–Kuhn–Tucker optimality conditions. All three approaches have successfully been tested giving the same result; however, the last one offers the most convenient analytical formulation. Using this approach the problem (5.8) may be reduced to the following compact form:

$$\begin{cases} z(\theta_2, \gamma_2) = 0 \\ 2\xi s(\theta_2, \gamma_2) + 1 = 0 \end{cases} \tag{5.10}$$

where  $z(\theta_2, \gamma_2)$  has already been defined in (5.5) and  $s(\theta_2, \gamma_2)$  is given by

$$\begin{aligned} s(\theta_2, \gamma_2) &= (\gamma_2 + 2\theta_2) s_1(\theta_2, \gamma_2) + \theta_2 s_2(\theta_2, \gamma_2) \\ &\quad - \sin \gamma_2 F_1(\gamma_2 + \theta_2, \theta_2) \end{aligned}$$

and

$$\begin{aligned} s_1(\theta_2, \gamma_2) &= \sin \gamma_2 F_0(\gamma_2 + \theta_2, \theta_2) \\ &\quad - \cos \gamma_2 F_1(\gamma_2 + \theta_2, \theta_2) \\ s_2(\theta_2, \gamma_2) &= -\sin \gamma_2 G_0(\gamma_2 + \theta_2, \theta_2) \\ &\quad + \cos \gamma_2 G_1(\gamma_2 + \theta_2, \theta_2) \end{aligned}$$

This is the system of two transcendental equations of two unknowns  $\theta_2$  and  $\gamma_2$ . Obviously, a lot of laborious algebraic transformations (not possible to be presented here) were needed to obtain so compact form of the problem. It should be pointed out that the solution of (5.10) is valid only for  $\xi \in [\xi_0, \xi_1]$ , where  $\xi_1$  is the upper limit value of  $\xi$  for the solution without the bottom bar NN' and  $\xi_0$  is the lower limit of  $\xi$  resulting from restriction of the feasible domain to the upper half-plane. The values of these limiting parameters will be given in the sequel.

### 5.3 Case 2: the optimal framework with the bottom bar NN'

Let us now proceed to the second case: the structure with the bottom bar NN'. The formula (5.1) is still valid, contrary to (5.4) which has to be neglected. The force  $Q_x$  is defined by (2.47) which after including (5.1), (5.3) and (5.5) may be rewritten as

$$Q_x = F_x z(\theta_2, \gamma_2) \tag{5.11}$$

The volume  $V_1$  of the structure RBDCNAR is given by (2.74) as before, but now  $Q_x \neq 0$  and the virtual work  $Q_x w_x(N)$  has to be included. The volume of bar DS is given by (5.6). Similarly, the volume of the bar NT is expressed by

$$V_3 = \frac{-Q_x}{\sigma_p} (L - d) \tag{5.12}$$

The sign (−) in this formula results from the observation that the displacement  $w_x(N)$  is positive, hence the bar  $NN'$  is under compression and the value of the force  $Q_x$  is negative. Formally, the magnitudes  $F_x$  and  $Q_x$  appearing in (5.6) and (5.12) should be replaced by their absolute values, but this would bring about a much harder to solve non-smooth problem. The volume  $2\bar{V} = 2V_1 + 2V_2 + 2V_3$  of the whole structure of Fig. 18 with the bottom bar  $NN'$  is expressed by

$$2\bar{V} = 2\bar{V} + 2V_0 \frac{\xi z(\theta_2, \gamma_2)}{\gamma_D} (\xi L - L + w_x(N)) \quad (5.13)$$

In the present case, the optimal structure is determined by the minimization problem without any constraints

$$\min_{\theta_2, \gamma_2} \bar{V}(\theta_2, \gamma_2) \quad (5.14)$$

which makes the solution procedure (either numerical or analytical) simpler than before. Nevertheless, the computation of the derivatives  $\frac{\partial \bar{V}}{\partial \theta_2}$  and  $\frac{\partial \bar{V}}{\partial \gamma_2}$  is still a very laborious task. An essential simplification of the problem formulation may be achieved from the following observation. The horizontal displacement of point T which lies on the symmetry axis of the whole structure (Fig. 18) should vanish or

$$d - L + w_x(N) = 0 \quad (5.15)$$

By (2.58) and (2.3) this condition may be written as

$$\xi \cos(2\gamma_2) + \xi - 1 = 0 \quad (5.16)$$

or

$$2\xi \cos^2 \gamma_2 - 1 = 0 \quad (5.17)$$

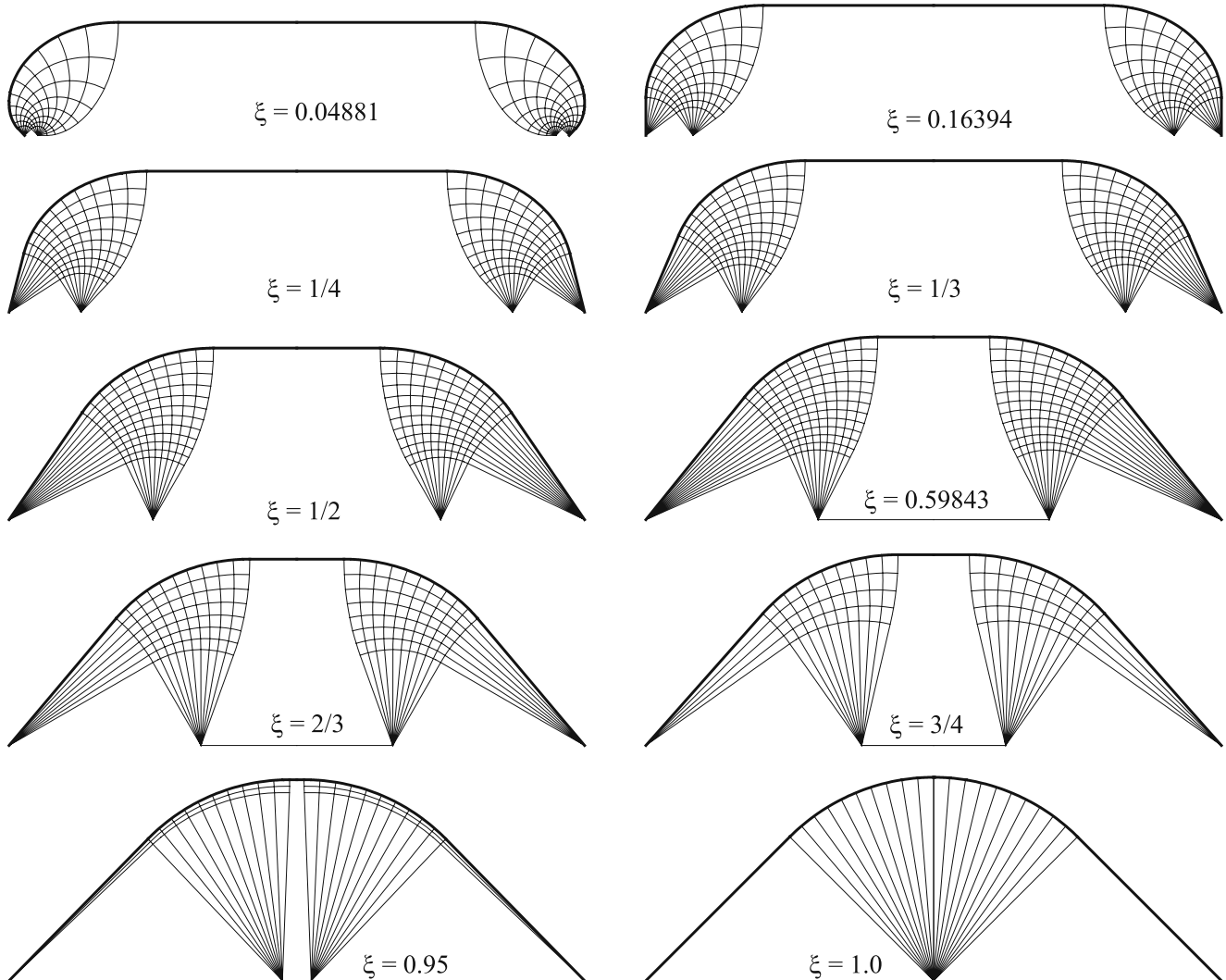


Fig. 20 Selected analytical solutions of problem of Fig. 16

Therefore, for the structure with the bottom bar NN' the angle  $\gamma_2$  directly depends on  $\xi$ —the relative position of applied load  $P$ . Note that the solution to these equations exist only for  $\xi \geq 1/2$ . The remaining unknown  $\theta_2$  may be derived from stationary conditions  $\frac{\partial V}{\partial \theta_2} = 0$  or  $\frac{\partial V}{\partial \gamma_2} = 0$ . The extensive exploration of this problem allowed us to obtain the possibly simplest system defining the optimal structure in the following form:

$$\begin{cases} 2\xi \cos^2 \gamma_2 - 1 = 0 \\ 2\xi s(\theta_2, \gamma_2) + 1 = 0 \end{cases} \quad (5.18)$$

*Remark* The attentive reader may at this moment be a little confused. Why the similar procedure of using displacement compatibility condition cannot be used for point S?

The reason is not so obvious. The displacements of the points D and N, defined in (2.58) and (2.73), were derived for arbitrary chosen rigid rotation of the framework RBDCNR around the point R. The displacement  $w_x(N)$  is parallel to the radius RN and is not sensitive to this rotation, hence the formula (2.58)<sub>1</sub> holds (in the infinitesimal sense of  $\psi$ ). Contrary, the displacements  $w_y(N)$  and  $w_x(D) = u_D$  are implicitly dependent on the parameter  $\psi$ , which was chosen to be equal  $-1$ . This assumption was motivated to

obtain the solution corresponding to this given by Chan (1966). It is possible to rearrange the formulae for displacements  $w_y(N)$  and  $w_x(D)$  by choosing the parameter  $\psi$  more suitably. However, it is not constant and depends on  $L$ ,  $\theta_2$  and  $\gamma_2$ . The final formulae obtained in this way are more complicated than (2.58) and (2.73) and will not be presented here.

### 5.4 Synthesis of the optimal layouts

The parameter  $\xi_1$  separating two cases of the solution has to satisfy simultaneously the conditions (5.4) and (5.16). It means that for  $\xi = \xi_1$  the bottom horizontal bar NN' appears to be visible. Thus we construct the system of three equations

$$\begin{cases} z(\theta_2, \gamma_2) = 0 \\ 2\xi_1 \cos^2 \gamma_2 - 1 = 0 \\ 2\xi_1 s(\theta_2, \gamma_2) + 1 = 0 \end{cases} \quad (5.19)$$

with three unknowns  $\xi_1, \theta_2, \gamma_2$ . As before the system is transcendental. Nevertheless it allows one to find numerical value of  $\xi_1 = 0.598426$ . For  $\xi \leq \xi_1$  the optimal structure is defined by (5.10) and for  $\xi \geq \xi_1$  by (5.18), respectively.

**Table 1** The solutions of problem of Fig. 16 for different values of  $\xi$

$\xi$	$\gamma_2$	$\theta_2$	$\theta_1$	$x_D/d$	$y_D/d$	$Q_x/P$	$F_x/P$	$2V/V_0$
0.04881	0.75994	1.57080	2.33074	0.34450	0.41529	0	0.11752	0.85915
0.05	0.75857	1.55696	2.31553	0.34463	0.41538	0	0.12037	0.87436
0.1	0.70214	1.17523	1.87738	0.36392	0.42718	0	0.23410	1.41828
0.16394	0.63881	0.93198	1.57080	0.40739	0.45210	0	0.36262	1.95512
0.2	0.60821	0.84399	1.45221	0.43602	0.46769	0	0.42763	2.21211
0.25	0.57120	0.75291	1.32411	0.47840	0.48983	0	0.51038	2.53184
0.3	0.53950	0.68473	1.22423	0.52280	0.51197	0	0.58598	2.81964
1/3	0.52083	0.64788	1.16871	0.55317	0.52656	0	0.63303	2.99762
0.4	0.48828	0.58848	1.07676	0.61515	0.55517	0	0.72050	3.32723
0.5	0.44871	0.52294	0.97166	0.71019	0.59638	0	0.83840	3.77092
0.59843	0.41759	0.47554	0.89313	0.80519	0.63491	$-2.2 \cdot 10^{-10}$	0.94254	4.16355
0.6	0.42053	0.47205	0.89258	0.80588	0.63520	$-0.00299$	0.94458	4.16953
2/3	0.52360	0.34689	0.87049	0.83617	0.64768	$-0.10942$	1.02932	4.40104
0.7	0.56394	0.29626	0.86021	0.85191	0.65389	$-0.15240$	1.07051	4.50303
0.75	0.61548	0.23017	0.84565	0.87599	0.66313	$-0.20885$	1.13100	4.64170
0.8	0.65906	0.17299	0.83205	0.90046	0.67223	$-0.25830$	1.19006	4.76534
0.9	0.72973	0.07760	0.80733	0.95005	0.68999	$-0.34281$	1.30437	4.97460
0.95	0.75907	0.03698	0.79605	0.97501	0.69863	$-0.37984$	1.35981	5.06287
0.99	0.78035	0.00713	0.78748	0.99500	0.70542	$-0.40753$	1.40341	5.12657
1	0.78540	0.00000	0.78540	1.00000	0.70711	$-0.41421$	1.41421	5.14159

The angles  $\gamma_2, \theta_2, \theta_1$  are given in radians



Now we are able to perform parametric study of the influence of the parameter  $\xi$  on the solution. The layouts of the optimal structures for selected values of  $\xi$  are shown in Fig. 20. More detailed results including the optimally chosen design variables are set up in Table 1. As was expected, the volume of the whole structure increases monotonically for growing  $\xi$ , see Fig. 21.

The height  $y_D$  as well as  $x_D$  and the magnitude of the force  $F_x$  also increase monotonically. Obviously the magnitude of the force  $Q_x$  equals zero if  $\xi \leq \xi_1$ , and then increases (in negative sense). It should be noted that the last solution for  $\xi = 1$  corresponds exactly to the well known solution given by Michell (1904), when  $\gamma_2 = \frac{\pi}{4}$ ,  $\theta_2 = 0$ ,  $\theta_1 = \frac{\pi}{4}$ ,  $x_D = 1d$ ,  $y_D = \frac{\sqrt{2}}{2}d$ ,  $F_x = \sqrt{2}P$  and  $2V = (\pi + 2)V_0$ . The force  $F_x$  is equal to the force in the upper cable (like for all other  $\xi$ ) but additionally we can discover that the limiting value of the magnitude of the force  $Q_x$  approaches  $(1 - \sqrt{2})P$  if  $\xi \rightarrow 1$ . The dependence of the angles  $\gamma_2$ ,  $\theta_2$  and  $\theta_1$  on  $\xi$  is more complicated, see Fig. 22. We can easily recognize two branches:  $\xi \leq \xi_1$ ,  $\xi \geq \xi_1$  of the optimal solution. The most interesting is the diagram of the angle  $\gamma_2$ , which decreases for  $\xi \leq \xi_1$ , and then increases up to the value of  $\pi/4$ . The smallest value of  $\gamma_2 = 0.41759$  (about  $24^\circ$ ) occurs at the sharp (non-smooth) minimum for  $\xi = \xi_1$ .

At the end of the discussion of the results presented in Table 1 it should be explained what are the two additional points, characterized by  $\xi = 0.04881$  and  $\xi = 0.16394$ . The first one relates to the lower limit  $\xi_0$  for which the solution obtained from (5.10) is applicable. For  $\xi$  lower than  $\xi_0$  the sum  $\gamma_1 + \theta_1$  is bigger than  $\pi$  and the solution of (5.10) goes beyond the assumed upper half-plane (see Fig. 16). This special and relatively rare case will not be investigated in this paper. We can however calculate the limiting value  $\xi_0$  from (5.10) treating it as the system of unknowns  $\xi$  and  $\gamma_2$ , and assuming  $\theta_2 = \pi/2$ . The last condition results from geometrical relations:  $\gamma_1 + \gamma_2 = \pi/2$  and (5.1). The point

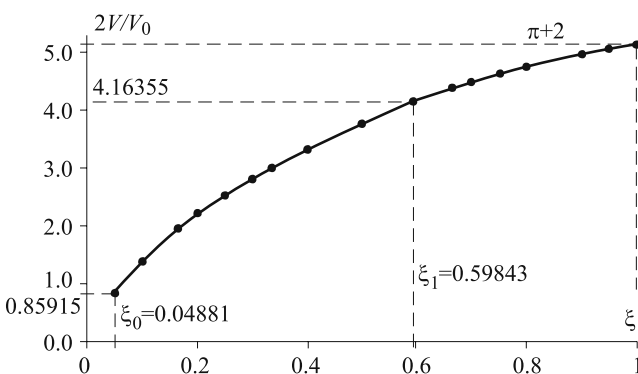


Fig. 21 The chart of optimal volume depending on  $\xi$

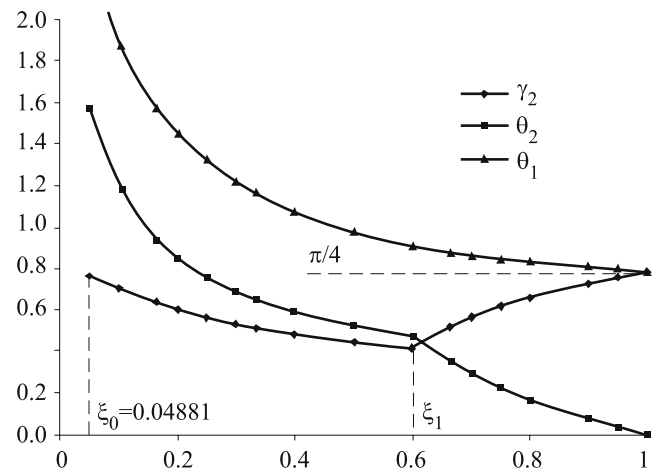


Fig. 22 The chart of  $\gamma_2$ ,  $\theta_2$ ,  $\theta_1$  (in radians) with respect to  $\xi$

$\xi = 0.16394$  refers to the solution for which the upper cable starts vertically from the supporting point R. This case was considered in similar way as before, using (5.10) with the obvious statement  $\theta_2 + \gamma_2 = \pi/2$ .

The values of the volume found by the numerical method proposed by Sokół (2010) are set up and compared with analytical solutions in Table 2. A lot of different densities of ground structures were tested. The calculations leading to the results given in Table 2 were performed using the ground structure of density  $L/100$  and internal connections of nodes up to distance of 15 cells. One notes that if the number of members is bigger than 1,000,000 the accuracy of the volume predictions remains below 1%. The linear formulation of the optimization problem assures the global minimum (in a discrete meaning), hence the layouts obtained in the numerical way are valuable hints of optimal frameworks, compare Figs. 17 and 20.

The analytical solutions shown in Fig. 20 do not have their counterparts in the literature. These solutions can only be compared with some truss layouts published in

Table 2 Comparison of the analytical and numerical solutions

$\xi$	$V_a/V_0$	$V_n/V_0$	err (%)
0.1	1.41828	1.42563	0.52
0.2	2.21211	2.21748	0.24
0.3	2.81964	2.82446	0.17
0.4	3.32723	3.33178	0.14
0.5	3.77092	3.77538	0.12
0.6	4.16953	4.17368	0.10
0.7	4.50303	4.50648	0.08
0.8	4.76534	4.76826	0.06
0.9	4.97460	4.97878	0.08
1.0	5.14159	5.14466	0.06

Achtziger (1997). These solutions can also be compared with optimal layouts of the continuum based topology optimization concerning distribution of one material within a given domain realizing minimization of the compliance. In particular, some of the Lógó et al. (2009) results compare favorably with the analytical solutions shown here. It is nevertheless difficult to justify the noted similarity, due to essential differences between the formulations: discrete and continuum. Some remarks towards understanding these two approaches can be found in the recent papers by Rozvany (2009, 2010).

## 6 Final remarks

The classical Michell structures are determined by the relevant Michell–Hencky nets being determined by the boundary conditions. The Michell-like cantilevers belong to this class. The characteristic feature of these solutions is that the Michell–Hencky nets are independent of the point loads applied. For instance, the net shown in Fig. 2 of Lewiński and Rozvany (2008b), concerning the problem of the exterior of the square, applies to many kinds of the point loads, as shown in this figure. Let us name this property as insensitivity of the Michell–Hencky net to the loading applied. This feature of insensitivity implies the superposition principle: the optimal structure subject to a given set of the admissible loads is formed by superimposing the optimal structures for the independent loads.

The mentioned property of insensitivity of the nets cease to hold in the problem considered. All the Michell–Hencky nets constructed in the present paper are determined both by the loading and the boundary conditions. Consequently, the solutions of Fig. 20 cannot be superimposed. For instance, the two solutions corresponding to two data sets  $(P_1, d_1)$ ,  $(P_2, d_2)$  do not determine the exact solution for the case of application of the four forces:  $P_1, P_2, P_2, P_1$ . The four forces problem should be solved separately. Such problems were only treated numerically, see Lógó et al. (2009).

Consequently, the case of the distributed vertical loading cannot be solved by superimposing the layouts found in Section 5, but necessitates a new analytical treatment. By now only some semi-inverse solutions are available, see papers by Hemp (1974) and Chan (1975), concerning a carefully selected class of the vertical distributed load along the line linking the supports. In particular, the important case of the constant loading along  $RR'$  has not been solved till now.

Lastly, let us note that the exact solutions found in Section 5 of the present paper, see Fig. 16, have not been substantiated by the theoretical construction of the kinematically admissible virtual displacement fields within the whole feasible domain, i.e. within the whole half-plane over

the line linking the supports. Some hints towards this issue can be found in Chan (1975), Rozvany (1998) and Melchers (2005), but the complete construction is still pending.

**Acknowledgments** The authors express their cordial thanks to Prof. Henry S.Y. Chan from Department of Mathematics of the City University of Hong Kong for having generously sent his, probably confidential, report of 1966 and drawing our attention to the open issues of the three forces problem. The problem of optimal designing of the symmetric frameworks considered was suggested to the second author by Prof. George Rozvany and Prof. Janos Lógó. This suggestion and encouragement is kindly acknowledged. The authors are also indebted to Prof. Peter Neumann (Düsseldorf) who drew our attention to the rarely cited paper by C. Carathéodory and E. Schmidt in which the crucial formulae for the Hencky–Prandtl nets determining geometry of Michell truss layouts were originally derived.

The present paper was prepared within the Research Grant no N506 071338, financed by the Polish Ministry of Science and Higher Education, entitled: *Topology Optimization of Engineering Structures. Simultaneous shaping and local material properties determination.*

**Open Access** This article is distributed under the terms of the Creative Commons Attribution Noncommercial License which permits any noncommercial use, distribution, and reproduction in any medium, provided the original author(s) and source are credited.

## References

- Achtziger W (1997) Topology optimization of discrete structures: an introduction in view of computational and nonsmooth aspects. In: Rozvany GIN (ed) Topology optimization in structural mechanics. Springer, Wien, pp 57–100
- Carathéodory C, Schmidt E (1923) Über die Hencky-Prandtschen Kurven. *Z Angew Math Mech* 3:468–475
- Chan ASL (1960) The design of Michell optimum structures. Rep. Coll. Aeronaut. Cranfield, no 142. The paper unavailable to the authors
- Chan HSY (1963) Optimum Michell frameworks for three parallel forces. The College of Aeronautics. Cranfield, Report AERO, no 67
- Chan HSY (1964) Tabulation of some layouts and virtual displacement fields in the theory of Michell optimum structures. The College of Aeronautics. Cranfield, CoA Note Aero, no 161
- Chan HSY (1966) Minimum weight cantilever frames with specified reactions. University of Oxford. Depart. of Eng. Sci. Eng. Laboratory, Parks Road, Oxford, June 1966, no 1,010.66, p 11 with 4 figures. The paper never cited before
- Chan HSY (1967) Half-plane slip-line fields and Michell structures. *Q J Mech Appl Math* 20:453–469
- Chan HSY (1975) Symmetric plane frameworks of least weight. In: Sawczuk A, Mróz Z (eds) Optimization in structural design. Springer, Berlin, pp 313–326
- Dewhurst P (2001) Analytical solutions and numerical procedures for minimum-weight Michell structures. *J Mech Phys Solids* 49: 445–467
- Gilbert M, Tyas A (2003) Layout optimization of large-scale pin-jointed frames. *Eng Comput* 20:1044–1064
- Golay F, Seppacher P (2001) Locking materials and the topology of optimal shapes. *Eur J Mech A, Solids* 20:631–644
- Graczykowski C, Lewiński T (2006a) Michell cantilevers constructed within trapezoidal domains—part I: geometry of Hencky nets. *Struct Multidisc Optim* 32(5):347–368

- Graczykowski C, Lewiński T (2006b) Michell cantilevers constructed within trapezoidal domains—part II: virtual displacement fields. *Struct Multidisc Optim* 32(6):463–471
- Graczykowski C, Lewiński T (2006c) Force fields within Michell-like cantilevers transmitting a point load to a straight support. In: Bendsøe M, Olhoff N, Sigmund O (eds) *IUTAM symposium on topological design optimization of structures, machines and materials. Status and perspectives. Solid mechanics and its application*, vol 137. Springer, Dordrecht, pp 55–65
- Graczykowski C, Lewiński T (2007a) Michell cantilevers constructed within trapezoidal domains—part III: force fields. *Struct Multidisc Optim* 33:27–46
- Graczykowski C, Lewiński T (2007b) Michell cantilevers constructed within trapezoidal domains—part IV: complete exact solutions of selected optimal designs and their approximations by trusses of finite number of joints. *Struct Multidisc Optim* 33:113–129
- Hemp WS (1973) *Optimum structures*. Clarendon Press, Oxford
- Hemp WS (1974) Michell framework for uniform load between fixed supports. *Eng Optim* 1:61–69
- Lewiński T, Rozvany GIN (2008a) Exact analytical solutions for some popular benchmark problems in topology optimization III: L-shaped domains. *Struct Multidisc Optim* 35:165–174
- Lewiński T, Rozvany GIN (2008b) Analytical benchmarks for topological optimization IV: square-shaped line support. *Struct Multidisc Optim* 36:143–158
- Lewiński T, Zhou M, Rozvany GIN (1994a) Extended exact solutions for least-weight truss layouts—part I: cantilever with a horizontal axis of symmetry. *Int J Mech Sci* 36:375–398
- Lewiński T, Zhou M, Rozvany GIN (1994b) Extended exact solutions for least-weight truss layouts—part II: unsymmetric cantilevers. *Int J Mech Sci* 36:399–419
- Lewiński T, Rozvany GIN (2007) Exact analytical solutions for some popular benchmark problems in topology optimization II: three-sided polygonal supports. *Struct Multidisc Optim* 33:337–349
- Lógó J, Ghaemi M, Rad MM (2009) Optimal topologies in case of probabilistic loading: the influence of load correlation. *Mech Des Struct Mach* 37(3):327–348
- McConnel RE (1974) Least-weight frameworks for loads across span. *J Eng Mech Div* 100:885–901
- Melchers RE (2005) On extending the range of Michell-like optimal topology structures. *Struct Multidisc Optim* 29:85–92
- Michell AGM (1904) The limits of economy of material in frame-structures. *Philos Mag* 8:589–597
- Rozvany GIN (1998) Exact analytical solutions for some popular benchmark problems in topology optimization. *Struct Optim* 15:42–48
- Rozvany GIN (2009) A critical review of established methods of structural topology optimization. *Struct Multidisc Optim* 37:217–237
- Rozvany GIN (2010) On symmetry and non-uniqueness in exact topology optimization. *Struct Multidisc Optim*. Accepted
- Sokół T (2010) A 99 line code for discretized Michell truss optimization written in Mathematica. *Struct Multidisc Optim*. Accepted